Photoluminescence of I-VII Semiconductor Compounds. Sensitized Luminescence from "Deep States" Recombination in CuBr/AgBr Nanocrystals

L. C. Hwang[a] (黃龍池), T. H. Wei[b] (魏台輝), Y. L. Hsia[a] (夏淵龍),
C. M. Li[a] (李俊明), P. L. Tu[a] (杜佩玲) and T. C. Wen[a]* (文在川)
[a]*Department of Medicinal and Applied Chemistry, Kaohsiung Medical University, Kaohsiung 802, Taiwan, R.O.C.*
[b]*Department of Physics, National Chung-Cheng University, Ming-Hsiung 621, Taiwan, R.O.C.*

The photoluminescence (PL) properties of CuBr and CuBr/AgBr semiconductor nanocrystals (NCs) embedded in borosilicate glasses are measured under band-to-band excitation by a 355-nm Nd:YAG laser. We observed emission from CuBr (peaked at 520 nm) doped glass, which is associated with deep states in CuBr NCs. We also observed the sensitized blue to orange-red emission in CuBr/AgBr-glass systems (peaked at 520 and 570 nm), in which the luminescence intensity of CuBr decreases with increasing AgBr concentrations, while it is enhanced significantly around 570 nm. The results are discussed by the possible energy transfer between them, or by the multi-exitonic recombination process which ejects an excited carrier from CuBr to AgBr NCs.

Keywords: CuBr and AgBr NCs; Photoluminescence; Energy transfer; Auger recombination.

INTRODUCTION

The preparation of light-emitting nanostructures based on semiconductor nanocrystals (NCs) has recently received considerable attention. For instance, efficient energy transfer from photo-excited smaller NCs (with higher energy states) to larger NCs (with lower energy states) has been found in a variety of III-V (e.g., InP[1]) and II-VI (e.g., CdSe[2]) compounds packed closely in solid films, and the kinetic rate of this energy transfer is fast, which is important for the realization of cascaded energy transfer devices based on NCs as well as on organic dyes.[3] However, there is no report for the sensitized luminescence of I-VII semiconductor compounds in the literature, as far as we know.

Simplified energy diagrams of a direct band-gap CuBr crystal ($E_g \approx 2.98$ eV at 80 K[4]) and a bulk AgBr having indirect band-gap ($E_g^{Indirect} \approx 2.7$ eV at 80 K[5]) are schematically depicted in Fig. 1. Under nitrogen laser excitation ($10^4 \sim 10^6$ W/cm^2 at 4 K), a radiative recombination of CuBr single crystals is composed mainly of *quasi* two-particle exciton (electron-hole) and biexciton processes,[6,7] whereas in bulk AgBr an additional phonon assisted process is necessary to provide momentum conservation.[8] On the other hand, quantum confinement of the indirect exciton in nano-size particles of AgBr causes admixture in the momentum space, and direct transition between the uppermost valence band maximum and the lowest conduction band minimum (i.e., between $L_{4,5}^-$ and Γ_6^+ which is ~2.7 eV apart as shown in Fig. 1) becomes partially allowed.[9] However, for our AgBr NCs embedded in glass with size distributions ranging from 3 ~ 15 nm, there is no emission observed in this

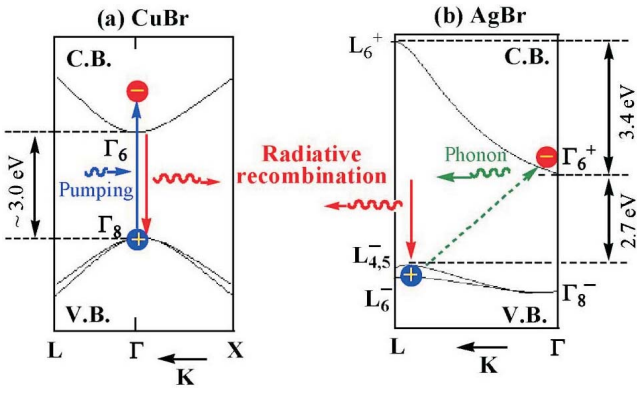

Fig. 1. Energy diagrams of (a) CuBr and (b) AgBr.

Dedicated to the memory of the late Professor Ho Tong-Ing.

* Corresponding author. E-mail: tschwe@kmu.edu.tw

work under band-to-band excitation. Therefore, the momentum selection rule may still remain significant. Also, nonradiative processes such as carrier ionization and Auger effects have been studied intensively in quantum sized semiconductor nanocrystals.[10-14] Phonon assisted electron tunneling in its surroundings has been demonstrated by the time-resolved measurements as discussed in the section of results and discussion.

In this paper we report PL properties of CuBr doped and CuBr-AgBr co-doped borosilicate glasses under band-to-band excitation. The observed emission spectrum for CuBr NCs is described as a deep state recombination, and the sensitized blue to orange red luminescence in CuBr/AgBr NCs is discussed by the possible energy transfer or ionization process which ejects an excited carrier from CuBr to a nearby AgBr NCs.

EXPERIMENTAL METHOD

CuBr, AgBr and CuBr/AgBr co-doped borosilicate glasses are prepared by a melt and heat-treatment method as described elsewhere.[15,16] Using high purity (≥ 99.9%) SiO_2, Na_2CO_3, H_3BO_3, $Al(OH)_3$, CuO, AgBr, NaBr, SnO and $AlF_3 \cdot 3H_2O$, most of the glass mixtures are prepared according to the compositions listed in Table 1. All the glass plates with ~ 3.0 mm in thickness are colorless and transparent.

Transmission electron microscopy (TEM) analysis is performed using a JOEL JEM-2000EXII. Samples for TEM are prepared by spreading glass powder upon a slide with copper grids, which is covered with carbon film (Formvar/Carbon 200 Mesh Cu) and used as support for this measurement. Photographs for these samples are shown in Fig. 2. A large amount of the nanocrystals appear as dark ball shapes with diameters $d_0 \approx 15 \sim 50$ nm for CuBr (see Fig. 2a), and $d_0 \approx 3 \sim 15$ nm for AgBr NCs (Fig. 2b). A TEM picture recorded upon the doubly doped sample is shown in Fig. 2c. The enlargement picture (Fig. 2d) exhibits clearly that several small particles (may be AgBr) interacting with a single, large particle (or cluster), which may be composed of a few nanocrystals of CuBr and AgBr mixture.

Absorption spectra of our samples are shown in Fig. 3a, where the normalized emission spectra are also plotted

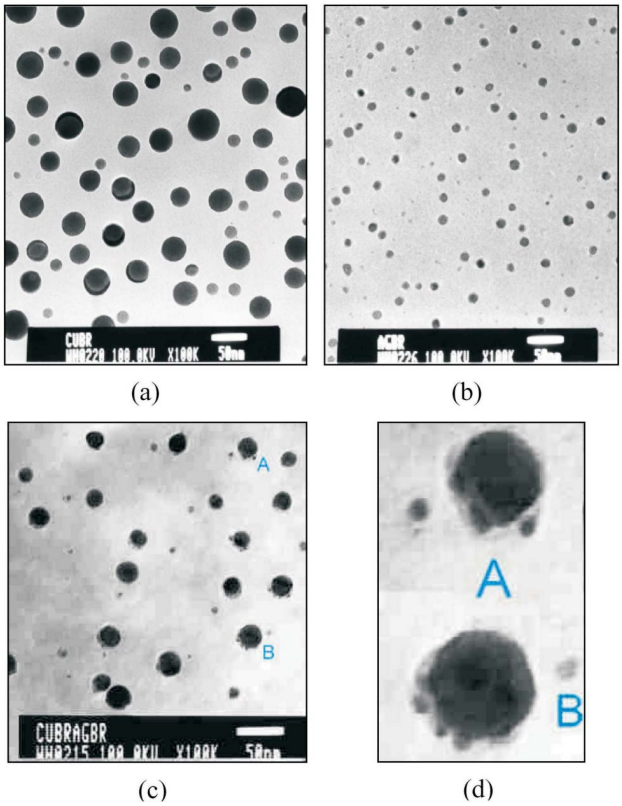

Fig. 2. TEM of glass samples with (a) 1.5mol%CuBr, (b) 1.6mol%AgBr, and (c,d) 0.78mol%CuBr-0.71mol%AgBr. Heat treatment conditions: annealing at 580 °C (10 h) for (a) and (b), and annealing at 570 °C (3 h) for (c) and (d).

Table 1. Calculated compositions (mol%) of glasses embedded with CuBr (1 and 7), CuBr/AgBr (2 to 5), and AgBr (6)

Number	Na_2O	Al_2O_3	B_2O_3	SiO_2	CuO	NaBr	AgBr	SnO	$AlF_3 \cdot 3H_2O$	Annealing conditions*
(1)	9.22	6.44	38.70	36.88	0.781	5.79		0.71	1.102	570 °C, 3 h
(2)	9.23	6.45	38.73	36.91	0.781	5.80	0.28	0.71	1.103	570 °C, 3 h
(3)	9.19	6.42	38.57	36.75	0.780	5.78	0.71	0.706	1.098	570 °C, 3 h
(4)	9.16	6.40	38.43	36.62	0.780	5.76	1.06	0.704	1.093	570 °C, 3 h
(5)	8.29	5.80	36.85	34.49	1.53	8.56	1.60	1.80	1.08	570 °C, 10 h
(6)	9.07	6.15	39.74	36.89		5.45	1.60		1.10	570 °C, 10 h
(7)	9.06	6.32	37.78	36.16	1.50	6.25		1.84	1.09	570 °C, 10 h

*Additional heat treatment is described individually in the text.

for comparison. The characteristic of size confinement effect in a CuBr/AgBr co-doped sample is shown in Fig. 3b, which displays that the absorption edge shifts toward longer wavelengths with increasing heat treatment time.

A Q-Switched Nd:YAG laser delivering linear polarized pulses at 355 nm wavelengths with ~6 ns pulse widths is employed as the excitation source. The luminescence spectra, collected in a direction of about 45° to that of the excitation pulses, are obtained by a 0.5-m grating monochromator (Acton SpectraPro-500) equipped with a photomultiplier (Hamamatsu R-928) whose output is fed into a digitizing oscilloscope. In order to obtain a good comparable luminescence intensity in different samples, the sample is set at the same place in the experimental setup, and the position and power of our irradiance and the width of the slit (~1.0 mm) to collect the emission light are fixed under the same conditions. The intensity of the luminescence spectrum from CuBr doped glass (centered at 520 nm) and from CuBr/AgBr co-doped glasses (centered at 520 and 570 nm) are calculated by integrating over each spectrum region.

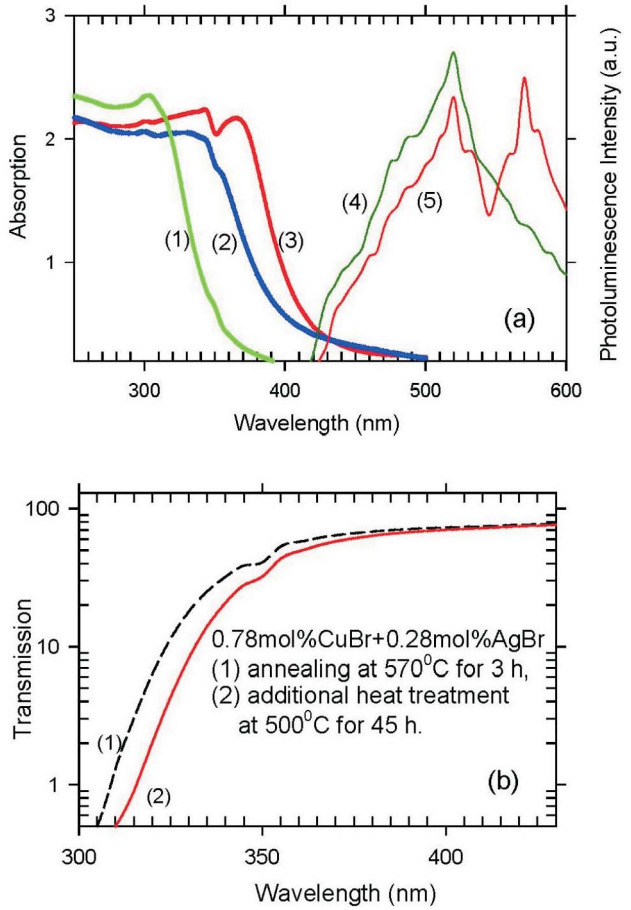

Fig. 3. Absorption spectra of glass samples with (1) 0.78mol%CuBr, (2) 0.78mol%CuBr/0.71mol% AgBr and (3) 1.6mol%AgBr. Normalized emission spectra of samples (1) and (2) are plotted as (4) and (5), respectively.

RESULTS AND DISCUSSION

Luminescence in CuBr nanocrystals

Recently, the luminescent properties of CuBr NCs ($d_0 \approx 12 \sim 82$ nm) embedded in a silicate glass were studied by Tamulaitis et al.[17] Under band-to-band excitation (quantum energy 3.15 eV, FWHM duration 5 ps), they obtained an emission spectrum ranging from 410 to 430 nm, and they attribute these radiative recombination processes to the exciton-exciton interaction and surface recombination.[17] This result corresponds with the literature report: CuBr crystal has been known to emit three bands at 2.945 eV (421.0 nm), 2.941 eV (421.6 nm) and 2.930 eV (423 nm), called M_f, M_T and M_L, by the irradiation of N_2 laser light at 4.2 K.[6-8] M_f, M_T and M_L bands are explained to originate from the annihilation of the biexcitons leaving excitons at the triplet, transverse and longitudinal states, respectively.

When the laser pulse is ≥ 3 μJ ($\approx 1.5 \times 10^4$ W/cm^2), we observe luminescence from a 1.5 mol% CuBr doped glass, and it becomes very bright at higher input intensity. This emission spectrum peaks at 520 nm as shown in Fig. 4(a), where an inset is its bright luminescence taken in the dark during the excitation at $E \approx 20 \pm 3$ μJ. We also find a linear relation between this peak intensity and the irradiance. Therefore, the emission spectrum depicted in Fig. 4(a) is likely to be caused by the radiative recombination associated with deep states such as interstitial copper-Cu_i, and these interstitial ions could be formed during the rapid cooling process of our glass samples. For example, deep center luminescence in the 0.7 eV spectra region is found by Krustok et al. in a direct gap II-VI compound CdTe:Cu:Cl, which is prepared by high-temperature melt followed by quenching to room temperature.[18] Since the rapid cooling promotes a formation of defects such as an interstitial Cu_i, they assume that the Cu_i is a deep donor and that it forms a DA pair with a deep acceptor on the Cd site. These DA pairs are responsible for the PL emission in the 0.7 eV spectra region.[17]

Sensitized luminescence in CuBr/AgBr nanocrystals

Although PL in nano-size particles of AgBr ($d_0 \approx 10 \sim 40$ nm) embedded in an inverse micelles system display free exciton emission peaking at 462 nm and a deep state recombination centered at 580 nm,[19] there is no detectable luminescence in the UV and visible region from our 1.6 mol% AgBr doped glass sample. However, when we irradiate a 0.03 mol% CuBr-1.6 mol% AgBr co-doped glass at $E \approx 5$ μJ (2.5×10^4 W/cm^2), its emission spectrum comprises two broad bands peaking at 520 and 570 nm. This luminescence intensity is enhanced dramatically by increasing the amount of CuBr concentrations as shown in Fig. 4(b); here we observe a strong PL from a 1.5 mol% CuBr-1.6 mol%

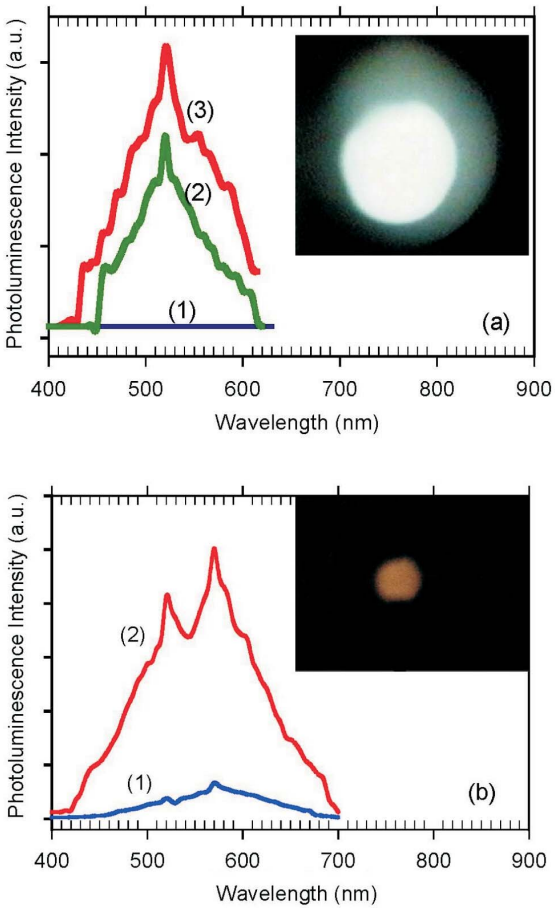

Fig. 4. (a) PL of a 1.5mol%CuBr doped glass excited at an average input energy (2) $E \approx 3.2$ μJ and (3) $E \approx 5.1$ μJ, an inset is taken in the dark when irradiated at $E \approx 20$ μJ, and (1) is a 1.6mol%AgBr doped glass irradiated at $E \approx 10.3$ μJ. (b) PL of (1) 0.03mol%CuBr-1.6mol%AgBr, and (2) 1.5 mol%CuBr-1.6mol%AgBr co-doped glasses. Both are irradiated at $E \approx 5$ μJ. An inset is taken in the dark during the excitation of (2).

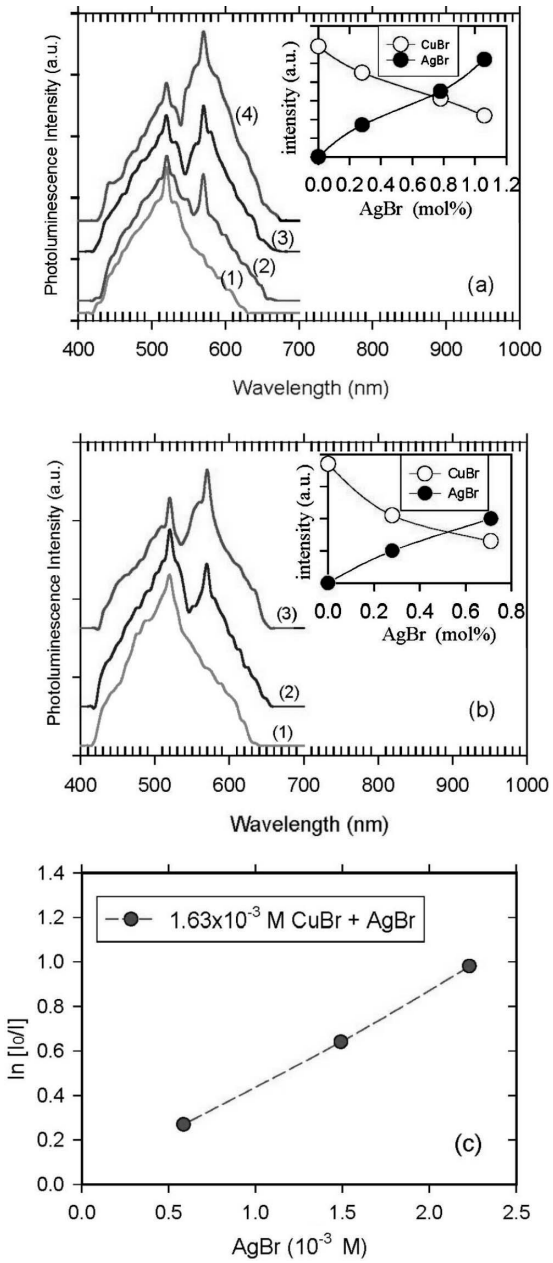

Fig. 5. (a) PL spectra from the samples of 0.78mol% CuBr/x-mol%AgBr co-doped glasses with (1) $x = 0$, (2) $x = 0.28$, (3) $x = 0.71$, and (4) $x = 1.06$ ($E \approx 10$ μJ (5×10^4 W/cm^2)). Inset is the change of integrated PL intensity as a function of co-dopant mole % of AgBr. (b) PL spectra of samples (1) to (3) in (a) with additional heat treatment at 500 °C for 45 hours ($E \approx 10.0$ μJ). Inset is the change of integrated PL intensity vs. mole% of AgBr. (c) A plot of $\ln(I_0/I)$ as a function of co-doped AgBr concentrations. I_0 and I are the intensities for CuBr emission in the absence and presence of AgBr, respectively. Data in this plot are taken from the results in (a).

AgBr co-doped glass consisting of two broad bands centered as before.

To understand the PL property in our CuBr/AgBr-glass system, we prepare several 0.78 mol% CuBr doped glasses which are co-doped with 0 to 1.06 mol% of AgBr, and their compositions are listed in Table 1 as numbers (1) to (4). When irradiated at $E = 10 \pm 0.3$ μJ ($(5 \pm 0.15) \times 10^4$ W/cm^2), we obtain a series of PL spectra from these samples; see Fig. 5(a). The intensity from our 0.78 mol%CuBr doped glass (centered at 520 nm) and from 0.78 mol% CuBr/AgBr co-doped glasses (centered at 520 and 570 nm individually) are calculated by integrating over each spectrum region. The variation of integrated PL intensity from the CuBr doped sample as a function of the codopant concentrations of AgBr is determined and displayed as an inset in Fig. 5(a). The emission of CuBr decreases with increasing AgBr concentration. At the same time, a significant enhancement of the AgBr emission is observed. With additional heat treatment at 500 °C for 45 hours of our samples (1) to (3), we obtain similar emission spectra as plotted in Fig. 5(b), where the inset exhibits the sensitized luminescent property as before. In summary, the above results indicate that (1) the observed emission spectrum centered at 520 and 570 nm is fairly constant for crystallites of various sizes and concentrations in the glass matrix and that it is consistent with the "deep states" recombination characterization, and (2) this PL could be caused by the energy transfer from CuBr into a nearby AgBr NCs.

Moreover, the Perrin formulation (Eq. 1), which assumes that an effective "quenching sphere" exists about the donor center molecule,[20] is applied to analyze the above experimental data.

$$\ln \frac{I_0}{I} \approx VN[C] \qquad (1)$$

In Eq. 1, I_0 and I are the intensities for donor (e.g., CuBr) emission in the absence and presence of an acceptor (e.g., AgBr), respectively, V is the volume of the active sphere (in cm^3), N is particle number density, and [C] is the concentration of acceptor in M.

A plot of $\ln(I_0/I)$ versus [C] is shown in Fig. 5c, where we obtain NV ≈ 7.4×10^{-22}, so that the radius R of the quenching sphere can be evaluated as $R = (3V/4\pi)^{1/3}$, the results of which give $R \approx (0.1 \sim 0.15) \times 10^{-12}$ cm for N ≈ $(17 \sim 4.6) \times 10^{16}$ cm^{-3}. The calculated values of R are much smaller than the radius of CuBr and AgBr NCs in our samples; that gives the efficiency of energy transfer $\Phi_{ET} \approx 1$.[19] However, in our system the entity from which energy is being transferred is a small particle with hundreds of AgBr molecules; therefore, it is not clear that eq. 1 can be properly applied here. We need further experiments (such as time resolved emission measurement) to confirm these energy transfer properties.

As schematically depicted in Fig. 6, we suggest that the free carriers are generated firstly in CuBr NCs through the pumping, while the excitons (and biexcitons) are formed rapidly and which can be captured by a deep state and followed by the radiative recombination. The energy transfer from CuBr to AgBr NCs is considered due to the dipole-dipole interaction between the donor-to-ground emission state in CuBr and the ground-to-excited states in AgBr NCs. The generated free carriers in AgBr NCs can undergo several different routes such as free exciton luminescence, or it can be captured by the deep states, which consist of a "donor site" (i.e. an interstitial Ag^+ for a Frenkel defect in the cation sub-lattice of AgBr[5,21]) and an "acceptor site" (i.e. silver ion vacancies), and then decayed radiatively as a donor-acceptor (D-A) recombination. Furthermore, as we described below, the observed sensitized PL could also be attributed to the ejection of an excited carrier from CuBr to a trap state of the nearby AgBr NCs.

Auger effects are expected to play an important role

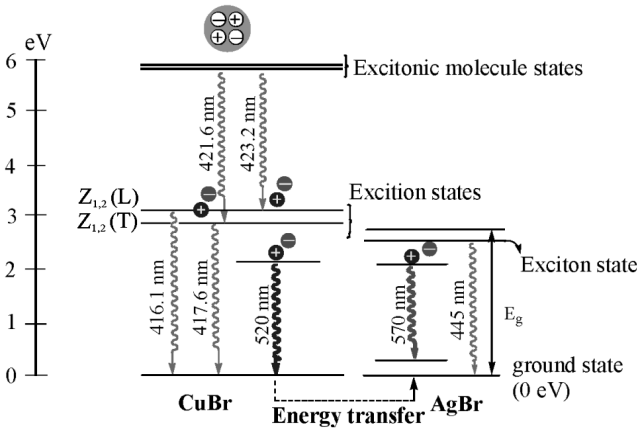

Fig. 6. Energy states of the exciton and excitonic molecule in CuBr crystals, and the optical transitions between them are measured by the irradiation of nitrogen laser at low temperature.[7] Emission from the CuBr doped and CuBr/AgBr co-doped samples observed in this work, and the possible energy transfer between CuBr and AgBr, are also drawn in this figure. Free exciton emission from the AgBr NCs is according to a literature report.[13]

in carrier relaxation.[10-14] For instance, earlier experiments demonstrate the following photon absorption and recombination pathways during the subpicosecond ultraviolet (UV) laser flash on small CdS ($d_0 \approx 2.5$ nm) or ZnCdS ($d_0 \approx 4.0$ nm) colloids:[10,11]

$$\text{Step 1: } (CdS)_n \xrightarrow{h\nu} (CdS)_n (e^- - h^+) \rightarrow (CdS)_n$$

$$\text{Step 2: } (CdS)_n (e^- - h^+) \xrightarrow{h\nu} (CdS)(e^- - h^+)_2 \rightarrow (CdS)_n (e^- - h^+)$$

$$\text{Step 3: } (CdS)(e^- - h^+)_2 \xrightarrow{\text{Auger recombination and electron scattering}} (CdS)_n (h^+) + (e^-)_{aq}$$

Since the energy of the first excited state (Step 1) is not high enough for an electron ejection, the electron emitted into the aqueous phase is therefore attributed to the doubly excited state, as Step 3. Because of the very large spatial overlap between the two electron-hole pairs in the small CdS and ZnCdS quantum dots, large amounts of hydrated electrons (i.e, about 30% as compared with the maximum electron yield) are produced after multiphoton excitation.[11]

More recently, time-resolved PL measurements are performed on thin films of dispersed core/shell CdSe/ZnS NCs by Krous et al.[14] Their results show that an excited carrier in the core NCs can be efficiently scattered to a trap state of the shell NCs via phonon-assisted tunneling due to increased carrier wave function overlap with the trap states. This excited carrier can be generated by a sequence of bi-excitonic and even higher excitonic Auger recombination processes as described in Ref. 14.

A possible carrier scattering pathway from the CuBr into AgBr NCs is schematically drawn in Fig. 7, where we proposed that an electron is ejected to a higher energy level through the bi-exciton Auger recombination. After that, this excited electron can relax thermally followed by recombining radiatively, while it can be scattered to a trap state which is located in the vicinity of AgBr NCs. Therefore, the interplay between Auger recombination and carrier ionization may increase the PL intensity in the AgBr NCs, and it may decrease the emission of CuBr in the meantime as observed in this work.

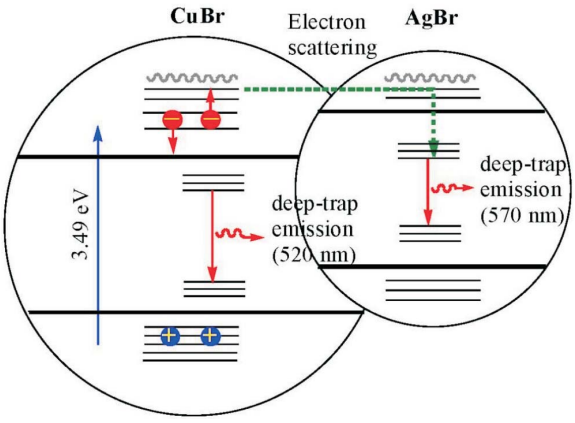

Fig. 7. Schematic description of the bi-exciton annihilation and carrier excitation followed by scattering to a trap state of AgBr surroundings via phonon assisted tunneling.

CONCLUSION

This work presents the luminescent properties of CuBr, AgBr and CuBr/AgBr nanocrystals embedded in borosilicate glasses when irradiated at 355 nm with input intensity ~10^5 W/cm^2. For the CuBr- and AgBr-doped samples, we only observe PL from the former which is peaked at 520 nm. Our CuBr/AgBr doubly doped samples exhibit blue to red emission, which is enhanced significantly by increasing the amount of CuBr NCs. In addition, for a series of doubly doped samples by varying the amounts of AgBr, the emission of CuBr decreases with increasing AgBr concentrations, while a significant enhancement of the AgBr emission is displayed at the same time. Possible energy transfer or carrier scattering from CuBr to AgBr NCs are proposed.

ACKNOWLEDGEMENTS

This work is supported by the National Science Council of Taiwan, ROC (NSC 94-2113-M-037-012).

Received July 31, 2006.

REFERENCES

1. Micic, D. I.; Jones, K. M.; Cahill, A.; Nozik, A. J. *J. Phys. Chem. B* **1998**, *102*, 9791.
2. Kagan, C. R.; Murray, C. B.; Nirmal, M.; Bawendi, M. G. *Phys. Rev. Lett.* **1996**, *76*, 1517.

3. Berggren, M.; Dodabalapur, A.; Slusher, R. E.; Ban, Z. *Nature* **1997**, *389*, 466.
4. Goldmann, A. *Phys. Stat. Sol*. (*b*) **1977**, *81*, 9.
5. Hamilton, J. F. *Adv. Phys.* **1988**, *37*, 359.
6. Grun, J. B.; Nikitin, S.; Bivas, A.; Levy, R. *J. Lumin.* **1970**, *12*, 241.
7. Suga, S.; Koda, T. *Phys. Stat. Sol.* (*b*) **1974**, *61*, 291.
8. Nakata, N.; Nagasawa, N.; Doi, Y.; Ueta, M. *J. Phys. Soc. Japan* **1975**, *38*, 903.
9. Kanzaki, H.; Tadakuma, Y. *Solid State Commun.* **1991**, *80*, 33.
10. Haase, M.; Weller, H.; Henglein, A. *J. Phys. Chem.* **1988**, *92*, 4706.
11. Kaschke, M.; Ernsting, N. P.; Muller, U.; Muller, H. *Chem. Phys. Lett*. **1990**, *168*, 543.
12. Regelman, D. V.; Dekel, E.; Gershoni, D.; Ehrenfreund, E.; Williamson, A. J.; Shumway, J.; Zunger, A. *Phys. Rev. B* **2001**, *64*, 165301.
13. Wang, L. W.; Califano, M.; Zunger, A.; Franceschetti, A. *Phys. Rev. Lett*. **2003**, *91*, 056404.
14. Kraus, R. M.; Lagoudakis, P. G.; Muller, J.; Rogach, A. L.; Lupton, J. M.; Feldmann, J.; Talapin, D. V.; Weller, H. *J. Phys. Chem. B* **2005**, *109*, 18214.
15. Chen, H.; Zhu, C.; Yu, B.; Lu, H.; Gan, F. *J. Non-Cryst. Solids* **2000**, *262*, 282.
16. Wei, T. H.; Wen, T. C.; Hwang, L. C.; Lee, S. L.; Chou, W. Y.; Hu, S. J.; Wang, J. H. *Opt. Mater.* **2006**, *28*, 569.
17. Tamulaitis, G.; Pakalnis, S.; Baltramiejunas, R. *J. Phys. Condens. Matter.* **1997**, *9*, 6771.
18. Krustok, J.; Collan, H.; Hjelt, K.; Madasson, J.; Valdna, V. *J. Lumi.* **1997**, *72-74*, 103.
19. Freedhoff, M. I.; Marchetti, A. P.; McLendon, G. L. *J. Lumin.* **1996**, *70*, 400.
20. Ermolaey, V. I. *Sov. Physic. Doklady* **1967**, *6*, 600.
21. von der Osten, W. *Physica B* **1987**, *146*, 240.